JACS
JOURNAL OF THE AMERICAN CHEMICAL SOCIETY
Article
pubs.acs.org/JACS

Solvation Effects on Transition Metal Hydricity

Charlene Tsay, Brooke N. Livesay, Samantha Ruelas, and Jenny Y. Yang*

Department of Chemistry, University of California, Irvine, California 92697, United States

Supporting Information

ABSTRACT: The free energy of hydride donation (hydricity) for $[HNi(DHMPE)_2][BF_4]$ (DHMPE = 1,2-bis-(dihydroxymethylphosphino)ethane was experimentally determined versus the heterolytic cleavage energy of hydrogen in acetonitrile, dimethyl sulfoxide, and water to be 57.4, 55.5, and 30.0 kcal/mol, respectively. This work represents the first reported hydricity values for a transition metal hydride donor in three different solvents. A comparison between our values and the hydricity of hydrogen and formate reveals a narrowing in the range of values with increasing solvent polarity. The thermochemical values also reveal solvation effects that impact the overall thermodynamic favorability of hydride generation from hydrogen and transfer to carbon dioxide. The quantitative solvation effects described herein have important consequences to the design and reactivity of catalysts for transformations that have hydride transfer steps throughout synthetic chemistry.

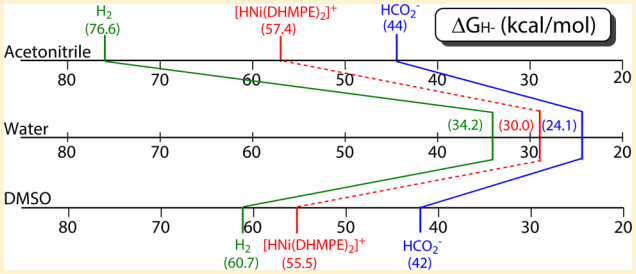

INTRODUCTION

Transition metal hydrides play a significant role in synthetic fuel forming (energy storage)[1−11] and fuel cell (energy utilization) reactions.[12−23] The rational design of energy efficient homogeneous catalysts for these reactions requires an understanding of the major bond making and breaking steps in order to avoid energetically inaccessible intermediates or thermodynamic sinks in the catalytic cycle. Transition metal hydrides are key redox catalyst intermediates in these reactions. As a result, the hydricities, or hydride donor strengths, (eq 1, ΔG_{H^-}) for many transition metal complexes in acetonitrile have been determined.[12,24−44] These quantitative determinations have demonstrated exceptional value in the design and optimization of catalysts for many reactions including proton reduction,[37,45−47] hydrogen oxidation,[16,48,49] formate oxidation,[18,20] and hydrogenation reactions,[9] but thus far their utility has been limited to reactions in acetonitrile.

$$\text{(eq 1)}\quad [HML]^n \rightleftharpoons [ML]^{n+1} + H^- \quad \Delta G_{H^-}$$

There is experimental evidence that metal hydride transfer to substrates such as CO_2 is strongly solvent dependent,[50−53] but a dearth of quantitative measurements to rationalize the reactivity patterns. For example, the hydricities of only two hydride donors have been measured in two different solvents.[54−56] We sought to improve the understanding of solvation effects by measuring the hydricity of a transition metal hydride in acetonitrile, dimethyl sulfoxide, and water to examine the effect of both solvent polarity and hydrogen bonding.

To accomplish this study, we synthesized a new nickel(II) bis(diphosphine) complex soluble in all three of our solvents of interest. Along with the Ni(II) complex, we independently synthesized and isolated the diamagnetic Ni(0) and Ni(II) hydride complexes, and utilized NMR spectroscopy to measure the equilibrium constants required to complete the thermodynamic cycles. The hydricity values presented herein were determined versus the hydricity of hydrogen (or free energy for heterolytic cleavage, ΔG_{H_2}) under standard state conditions. Measuring hydricity versus ΔG_{H_2} is convenient for establishing the thermodynamic requirements for generating the metal hydride from hydrogen and its subsequent stability toward protonation. This work represents the first time ΔG_{H^-} has been experimentally determined for a transition metal hydride donor in three different solvents.

Our values were compared to the hydricity of formate and revealed a narrowing in the range of hydricity values as the solvent polarity increases. However, the values did not track in a linear fashion. As a result, the nickel hydride becomes a much stronger hydride donor relative to formate in water. This is a compelling effect since it indicates hydride transfer from a transition metal to CO_2 or other substrates can become more thermodynamically favorable under benign aqueous conditions than in organic solvents.

Our analysis highlights the effect of solvation on the hydricity of our complex relative to that of formate, since the latter's value is known in all three of our solvents of interest. However, the trend of increasing hydride donor strength that corresponds with increasing solvent polarity is likely to have an impact on the broad scope of synthetic reactions that involve formal transfer of a hydride. Additionally, our experimentally determined thermochemical data are essential as benchmarks for improving solvation models in the computational determination and prediction of hydricity.[57−63]

Received: July 29, 2015
Published: October 14, 2015

DOI: 10.1021/jacs.5b07777
J. Am. Chem. Soc. 2015, 137, 14114−14121

RESULTS AND DISCUSSION

Synthesis and Characterization of $[Ni(DHMPE)_2][BF_4]_2$, $Ni(DHMPE)_2$, and $[HNi(DHMPE)_2][BF_4]$. Two different syntheses of the ligand 1,2-bis(dihydroxymethylphosphino)-ethane (DHMPE) have been previously reported, the first of which used K_2PtCl_4 to promote the reaction.[64] The other synthesis, published by Tyler and co-workers,[65] determined that the Pt salt was unnecessary. In our modified preparation, paraformaldehyde was added to 1,2-bis(phosphino)ethane in ethanol and the reaction mixture was heated to 80 °C for 24 h. The solvent was removed under vacuum and the remaining solid was washed with diethyl ether and redissolved in ethanol. After filtering, the solvent was removed from the filtrate under vacuum to afford DHMPE as a white solid.

$[Ni(DHMPE)_2][BF_4]_2$ (**1**, Scheme 1) was synthesized by reacting two equivalents of the DHMPE ligand with

Scheme 1. Synthesis of DHMPE Nickel Complexes

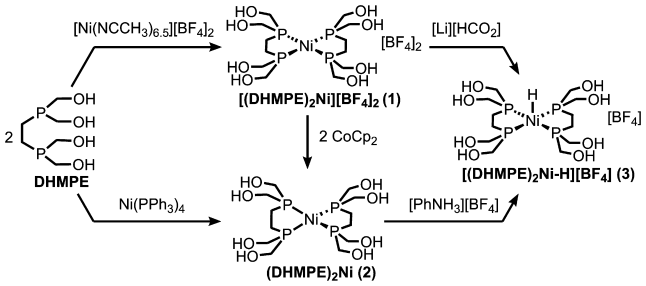

$[Ni(NCCH_3)_{6.5}][BF_4]_2$ in CH_3CN. The resulting orange solution was filtered and the solvent was removed under vacuum. The remaining orange residue was triturated with diethyl ether to yield **1** as a yellow-orange solid. Compound **1** exhibits a single phosphorus resonance in CD_3CN, DMSO-d_6, and D_2O (Table 1). The chemical shift in water is in

Table 1. ^{31}P NMR Resonances Referenced to H_3PO_4 of DHMPE Nickel Complexes in Various Solvents

complex	^{31}P NMR chemical shifts (ppm)		
	DMSO-d_6	CD_3CN	D_2O
$[Ni(DHMPE)_2][Cl]_2$[a]	n/a	n/a	65.1
$[Ni(DHMPE)_2][BF_4]_2$ (**1**)[b]	66.8	67.1	65.2
$Ni(DHMPE)_2$ (**2**)[b]	55.8	insol.	53.8
$[HNi(DHMPE)_2][BF_4]$ (**3**)[b]	57.5	55.6	54.7

[a]Reference 65. [b]This work.

agreement with that of the previously reported $[Ni(DHMPE)_2][Cl]_2$.[65] Further characterization by NMR spectroscopy is shown in Figures S1–S3 in the Supporting Information. Single crystals suitable for analysis by X-ray crystallography were grown by layering diethyl ether on a saturated acetonitrile solution. The solid-state structure, shown in Figure 1, reveals a 5-coordinate nickel center with an axially bound acetonitrile molecule. Selected metrical parameters are shown in Table 2; additional details are shown in Tables S2–S6 in the Supporting Information. The pseudosquare pyramidal nickel center has a τ_5 parameter of 0.067, where a value of 0 represents an ideal square pyramid and a value of 1 represents an ideal trigonal bipyramid.[66] One intramolecular, interligand hydrogen bond is observed between a hydroxyl hydrogen atom on one ligand and a hydroxyl oxygen atom on

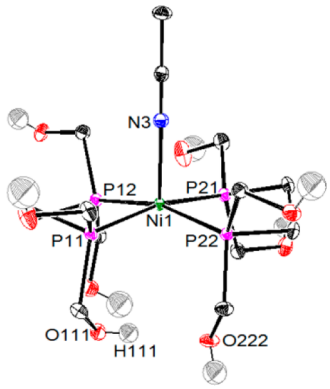

Figure 1. Solid-state structure of **1**. Thermal ellipsoids drawn at 50% probability including ligand hydroxyl hydrogens, which were located in the difference map and freely refined. Other hydrogen atoms and BF_4 anions omitted for clarity.

Table 2. Selected Bond Lengths (Å), Angles (deg), and τ_5 value for Solid-State Structure of 1

Ni1–P11	2.2086(4)	P11–Ni1–P12	84.324(16)
Ni1–P12	2.2270(4)	P21–Ni1–P22	84.564(16)
Ni1–P21	2.2123(4)	P11–Ni1–P22	93.005(16)
Ni1–P22	2.2094(4)	P12–Ni1–P21	94.760(16)
Ni1–N3	2.0973(13)	P11–Ni1–P21	167.987(17)
Ni1–P_4 plane	0.2699(3)	P12–Ni1–P22	163.953(17)
O222··H111	2.09(2)	O111–H111··O222	158(2)
		τ_5	0.067

the other ligand, while the other hydroxyl hydrogen atoms are involved in intermolecular hydrogen bonding with neighboring ligand hydroxyl oxygen atoms or counteranion fluorine atoms. While only one intramolecular hydrogen bond is present in the solid state, the hydroxyl hydrogen atoms observed in solution via ^1H NMR spectroscopy are chemically equivalent, indicating that their hydrogen bonds exchange rapidly in solution.

The nickel(0) complex, $Ni(DHMPE)_2$ (**2**), was synthesized either by reaction of DHMPE with $Ni(PPh_3)_4$ or by reduction of **1** with two equivalents of $CoCp_2$, as shown in Scheme 1. A single phosphorus resonance is observed for **2** in both DMSO-d_6 and D_2O (Table 1, Figures S6–S8). When dissolved in water, **2** is protonated by the solvent over the course of hours and results in the corresponding hydride $[HNi(DHMPE)_2]^+$ (**3**, *vide infra*). Unlike **1**, neutral complex **2** is insoluble in acetonitrile, benzonitrile, and tetrahydrofuran.

The nickel(II) hydride complex $[HNi(DHMPE)_2][BF_4]$ (**3**) was also synthesized by two different methods. The first method proceeds via protonation of the nickel(0) complex (**2**) in water by an equivalent of $[PhNH_3][BF_4]$. The second method to prepare **3** is through β-hydride elimination from a transient nickel(II)-formate species. In DMSO, the reaction of **1** with $[Li][HCO_2]\cdot H_2O$ proceeds rapidly, with no observed intermediates, to form **3**. The diamagnetic nickel hydride (**3**) has been characterized by ^1H and ^{31}P NMR spectroscopy (Figures S10–S12). The hydride resonance in the ^1H NMR spectrum is not observed in water, likely due to rapid proton exchange or hydrogen bonding, but is identifiable as a quintet in DMSO-d_6 (−13.43 ppm), CD_3CN (−13.47 ppm), and CD_3OD (−13.37 ppm).

Electrochemical Studies of $[Ni(DHMPE)_2][BF_4]_2$. The electrochemistry of the Ni(II) complex (**1**) in DMSO exhibits an irreversible reduction at −1.28 V and an oxidation wave at

DOI: 10.1021/jacs.5b07777
J. Am. Chem. Soc. 2015, 137, 14114–14121

−0.98 V versus the $FeCp_2^{+/0}$ couple at a scan rate of 25 mV/s, shown in Figure 2. For both events, a linear dependence on current versus the square root of the scan rate is observed, denoting diffusion control of the analyte at the electrode (Figure S4). No further reductive events are observed positive of −2.5 V versus $FeCp_2^{+/0}$. Electrochemistry of the Ni(0) complex (**2**) under the same conditions reveals an oxidation wave close to the potential of the return oxidation of **1** (Figure S9), indicating that the reductive wave at −1.28 V is a 2 e^- wave that reduces the Ni(II) complex to the Ni(0).

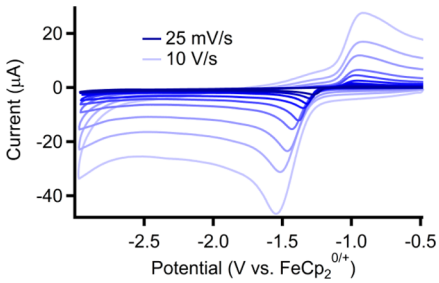

Figure 2. Cyclic voltammetry of **1** in DMSO. 3 mM analyte in 0.2 M $[Bu_4N][BF_4]$ solution with internal ferrocene reference. Potentials reported versus the $FeCp_2^{0/+}$ couple. Glassy carbon working and auxiliary electrodes; Ag/Ag^+ pseudoreference electrode. Scan rates range from 25 mV/s (darkest trace) to 10 V/s (lightest trace).

The two electron couple between the Ni(II) and Ni(0) species, as well as its irreversibility, may be attributed to the change in coordination geometry from square planar to tetrahedral upon reduction. The X-ray crystal structure of the Ni(II) complex (**1**) indicates intramolecular hydrogen bonding between the hydroxyl functionalities of the two phosphine ligands. These hydrogen bonds likely persist in nonprotic solvents such as DMSO. The change in coordination geometry upon reduction would require cleavage of the hydrogen bonds between the two ligands, which likely results in the observed shift in the reduction potential to a value more negative than that of the Ni(I/0) couple, resulting in net 2 e^- transfer. The rearrangement of the hydrogen bonds associated with the geometry change may also be the source of the irreversible nature of this reduction even though the Ni(0) complex (**2**) is stable and isolable. Electrochemical studies in acetonitrile (Figure S5) were complicated by the insolubility of the 2 e^- reduced complex, **2**.

Thermodynamic Determinations. The most direct method of measuring the hydricity is to use a square scheme that includes the 2 e^- reduction potentials of the metal, the pK_a of the metal hydride, and the free energy to reduce a proton to a hydride in the respective solvent (see the Supporting Information).[67] Since the redox event observed in our solvents of interest is irreversible, an exact value for $E_{1/2}$ of the Ni(II/0) couple cannot be determined. The potential of the reductive wave, however, can be used to calculate the lower bound for the hydricity, which is described in the SI.

(eq 2) $[ML]^{n+1} + B + H_2 \rightleftharpoons [HML]^n + [HB]^+$

$$\Delta G\ (\text{kcal/mol}) = \Delta G_{H2} - \Delta G_{H^-} - 1.37 * pK_{a(HB)}$$

To more accurately determine the hydricities (ΔG_{H^-}), we used the thermodynamic cycle shown at the top of Scheme 2. This method benchmarks the hydricity to the heterolytic cleavage energy of hydrogen (ΔG_{H_2}). This is a useful standard

Scheme 2. Methods Used to Determine Hydricity in Water, DMSO, and Acetonitrile

Heterolytic Cleavage of H_2

HM + BH ⇌	$M^+ + B^- + H_2$	-1.37 log(K_{eq})	(eq 3)
$B^- + H^+$ →	BH	-1.37 pK_a	(eq 4)
H_2 →	$H^+ + H^-$	$\Delta G°_{H2}$	(eq 5)
HM →	$M^+ + H^-$	$\Delta G°_{H^-}$ (kcal/mol)	(eq 6)

Hydride Transfer

HM + A^+ ⇌	M^+ + AH	-1.37 log(K_{eq})	(eq 7)
AH →	$A^+ + H^-$	$\Delta G°_{H^-(AH)}$	(eq 8)
HM →	$M^+ + H^-$	$\Delta G°_{H^-}$ (kcal/mol)	(eq 9)

to determine the reaction conditions necessary to generate the metal hydride from hydrogen and its stability toward protonation using eq 2. For example, eq 2 can be used with ΔG_{H^-} and ΔG_{H_2} in the appropriate solvent to determine the strength of base (by the pK_a of its conjugate acid) necessary to form the hydride from hydrogen. Conversely, eq 2 can be used to determine the acid strength necessary to protonate the metal hydride to form hydrogen. These relationships can be applied to optimize reaction conditions in stoichiometric and catalytic reactions, maximizing the utility of the thermochemical values reported. In addition to measuring the hydricity, we were also able to estimate the pK_a of hydride complex **3** in water and dimethyl sulfoxide.

Water. The aqueous hydricity was experimentally determined using a thermodynamic cycle that utilizes the heterolytic bond cleavage energy of H_2 (eq 5), shown in Scheme 2. This determines hydricity with respect to that of H_2. Different values for H_2 cleavage in water have been reported for various standard states.[54−56,67,68] In our analysis, we use the most recently reported value of 34.2 kcal/mol, which defines the standard state as 1 atm H_2.[69] This can be used in conjunction with the equilibrium constant of eq 3 and the pK_a of the respective acid (eq 4) to calculate the hydricity of the metal hydride.

The hydride complex **3** was generated cleanly *in situ* by adding an equivalent of the acid $[PhNH_3][BF_4]$ (pK_a = 4.6)[70] to the Ni(0) complex **2**. Additional equivalents of $[PhNH_3][BF_4]$ set up an equilibrium (eq 3) between the hydride (**3**) and the protonation products (**1** and H_2) under 1 atm of H_2, which is the standard state. The relative amounts of **1** and **3** were determined by ^{31}P NMR spectroscopy and the resulting K_{eq} of 0.03 was used to calculate a ΔG_{H^-} of 30.0 kcal/mol for hydride **3** in water. The solutions were monitored for at least 48 h to ensure the reactions had achieved equilibrium. More details on all of the thermodynamic calculations are provided in the Supporting Information.

In order to confirm that the system was at equilibrium, the reaction was initiated in the reverse direction. Accordingly, various equivalents of aniline were added to Ni(II) complex **1** under 1 atm of H_2 in order to partially generate hydride **3**. Though the relative concentrations of **1** and **3** appeared to reach equilibrium to give a ΔG_{H^-} value of 27.5 kcal/mol, a small amount of decomposition was observed, likely due to slow deprotonation of dicationic **1**, which has more acidic hydroxyl functionalities than monocationic **3**. The ΔG_{H^-} value obtained by this method is thus likely to be less reliable than the value determined above. However, establishing a similar equilibrium in the reverse direction validates our choice of acid/base (pK_a) and confirms the accuracy of our method.

DOI: 10.1021/jacs.5b07777
J. Am. Chem. Soc. 2015, 137, 14114−14121

We were also able to estimate the pK_a of the hydride of $[HNi(DHMPE)_2][BF_4]$ (**3**) in H_2O. Dissolution of $[Ni(DHMPE)_2]$ (**2**) in D_2O results in a broad peak at 53.8 ppm in the ^{31}P NMR spectrum (Figure S8). Over the course of hours, the signal sharpens and shifts to a singlet at 54.7 ppm, which matches the independently prepared nickel hydride complex **3**. The K_{eq} of the nearly complete protonation of the nickel(0) complex **2** by water (pK_a = 15.74)[71] to form hydride **3** was estimated to be 0.719, which translates to a pK_a of 15.6 or higher for hydride **3**.

Dimethyl Sulfoxide. The hydricity of **3** in DMSO was determined by the same method used for water. In order to determine the equilibrium constant for eq 3, complex **3** was generated *in situ* by the addition of one equivalent of $[PhNH_3][BF_4]$ (pK_a = 3.6)[72−74] to the nickel(0) compound **2**. Additional equivalents of $[PhNH_3][BF_4]$ were then added to establish the equilibrium in eq 3 under 1 atm of H_2. Using the value of 60.7 kcal/mol for the heterolytic bond cleavage energy of H_2 in DMSO,[67] ΔG_{H^-} was determined to be 55.6 kcal/mol. As in water, the equilibrium was also established in the reverse direction. Varying equivalents of $PhNH_2$ were added to compound **1** under 1 atm of H_2, and the K_{eq} was determined using the relative concentrations of **1** and **3** upon reaching equilibrium. This measurement resulted in a ΔG_{H^-} of 55.4 kcal/mol and an overall average of 55.5 kcal/mol.

The pK_a of the hydride $[HNi(DHMPE)_2][BF_4]$ (**3**) was determined to be 9.26 by adding various amounts of $[HNEt_3][BF_4]$ (pK_a = 9.0)[74,75] to **2** and establishing an equilibrium with **3**.

Acetonitrile. While the DHMPE ligand imparts water-solubility to the dicationic Ni(II) complex **1**, it renders the neutral Ni(0) complex **2** insoluble in both acetonitrile and benzonitrile. This property prevents *in situ* generation of metal hydride **3** by protonation of **2** and determination of its pK_a in acetonitrile. We were, however, able to determine K_{eq} for eq 3 by approaching the equilibrium from the reverse direction. Varying equivalents of aniline (anilinium, pK_a = 10.62)[26] were added to compound **1** under 1 atm of H_2. A K_{eq} of 0.54 was determined from the relative concentrations of **1** and **3**, resulting in a ΔG_{H^-} value of 57.4 kcal/mol.

An alternative method of measuring hydricity, via hydride transfer reactions with donors of known hydricity (Scheme 2), was also used in order to confirm that the hydricity value determined for **3** was consistent with other acetonitrile hydricity values reported in the literature. The hydricities of the other complexes used (Table 3) were also determined with

Table 3. Reported Hydricity Values in Acetonitrile vs H_2

compd	ΔG_{H^-} in CH_3CN (kcal/mol)	ref
$[HNi(depp)_2][PF_4]$	67.2, 66.2[a]	24
$[HNi(PNP)_2][PF_4]$	66	12

[a]Two different methods used to calculate ΔG_{H^-}.

respect to the heterolytic cleavage energy of H_2, the standard used for the hydricity values reported in this work. The 5-coordinate, square-pyramidal Ni(II) hydrides $[HNi(PNP)_2][BF_4]$ and $[HNi(depp)_2][BF_4]$ (PNP = $Et_2PCH_2N(CH_3)CH_2PEt_2$, depp =1,3-bis(diethylphosphino)propane) both have hydricities of about 66 kcal/mol. Upon mixing one equivalent of either of these hydrides with one equivalent of the Ni(II) complex **1**, no hydride transfer is observed. Assuming a minimum of 1% hydride transfer would be observable by either ^1H or ^{31}P NMR spectroscopy, this places an upper bound of about 63 kcal/mol on the hydricity value of **3**, which is consistent with the value obtained from the equilibrium measurements described above. These relative values are consistent with previously determined hydricity trends in acetonitrile. The two-atom backbone of the DHMPE ligand should impart a smaller bite-angle and thus lower hydricity value than the three-atom backbones of the PNP and depp ligands.[26]

In acetonitrile, the divalent compound **1** is unstable to strong bases. An insoluble product forms upon addition of one equivalent of either triethylamine (triethylammonium pK_a = 18.8)[76] or DBU (DBU = 1,8-diazabicycloundec-7-ene $HDBU^+$ pK_a = 24.34)[76] to **1** in CD_3CN, though some **1** remains in solution as observed by ^1H and ^{31}P NMR spectroscopy. Upon addition of two equivalents of DBU, complete precipitation occurs, **1** is no longer observed, and $HDBU^+$ is observed in the ^1H NMR spectrum. We propose that this is a result of double deprotonation of two hydroxyl groups on **1** to form a six-coordinate insoluble product, shown in Scheme 3. If the

Scheme 3. Proposed Decomposition Pathway for 1 in the Presence of Strong Base in CH_3CN

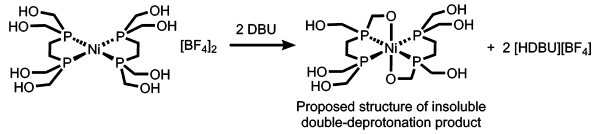

proposed product is correct, the inability to isolate a singly deprotonated complex suggests that the second deprotonation of **1** is more favorable than the first (i.e., lower pK_a) due to the formation of the proposed stable, neutral, six-coordinate compound. A much weaker base such as aniline (anilinium pK_a = 10.6)[76] does not react with **1**, while some interaction is observed with pyridine (pyridinium pK_a = 12.5)[76] and slow precipitate formation is observed with 2,6-lutidine (2,6-lutidiunium pK_a = 14.13).[76] The pK_a of the first deprotonation of the hydroxyl groups of **1** in acetonitrile is therefore estimated to be approximately 13.

Comparing Hydricity by Solvent. The ΔG_{H^-} values of **3** determined herein are summarized in Table 4 and Scheme 4

Table 4. Select ΔG_{H^-} Values (kcal/mol) in H_2O, CH_3CN, and DMSO and Their Respective Dielectric Constants (ε)

compd	H_2O (80)	CH_3CN (37)	DMSO (47)
H_2	34.2[a]	76.6[b]	60.7[b]
HCO_2^-	24.1[a]	44[c]	42[d]
$[HNi(DHMPE)_2]^+$	30.0[e]	57.4[e]	55.5[e]
$[HRu(\eta^6\text{-}C_6Me_6)(bpy)]^+$	22.2[f]	54[g]	
$[HRu(tpy)(bpy)]^+$	13.8[f]	39[g]	

[a]Reference 69. [b]Reference 67. [c]Reference 7. [d]Reference 50. [e]This work. [f]Reference 55. [g]Reference 54

along with the published values for the hydricity of hydrogen[67,69] and formate.[7,10,56] The hydricity of HCO_2^- in DMSO is estimated by extrapolating equilibrium data from a hydrogenation reaction to our standard state conditions.[50] The two prior complexes with reported hydricity values in CH_3CN and H_2O are also included, with the aqueous values adjusted

DOI: 10.1021/jacs.5b07777
J. Am. Chem. Soc. 2015, 137, 14114−14121

Scheme 4. Graphical Representation of Data from Table 4 (Adapted from ref 54)

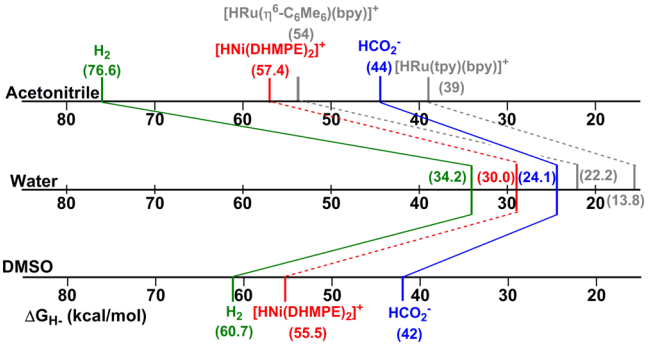

for the value of ΔG_{H_2} used in our calculation.[69] A lower ΔG_{H^-} indicates a stronger hydride donor.

A striking trend from our data is the powerful influence solvent polarity has on decreasing the span of hydricity values. Heterolytic bond cleavage free energies typically display large changes in magnitude by solvent since the resulting products are charged ions and their relative stability is strongly dependent on the polarity of their solvation spheres. In contrast, homolytic bond cleavage results in products of similar charge, and the stability of the bond cleavage products are not as strongly influenced by the dielectric constant, resulting in much smaller changes in free energies by solvent.[67] Our data quantifies the formidable impact polar solvents have on the free energy of reaction pathways that proceed via heterolytic bond cleavage.

Another noteworthy observation is the dramatic change in relative hydricity between the metal hydride complexes and formate, the product of hydride transfer to CO_2. These changes influence the reaction favorability for hydride transfer to CO_2 by solvent, particularly in water. Although dimethyl sulfoxide has a greater dielectric constant than acetonitrile, the free energy of hydride transfer $[HNi(DHMPE)_2]^+$ to CO_2 is unfavorable by about the same amount (13.4 and 13.5 kcal/mol for DMSO and acetonitrile, respectively). In contrast, the free energy for the same hydride transfer reaction is only unfavorable by 5.5 kcal/mol in water. The nonlinear changes in hydricity by solvent is also observed with $[HRu(\eta^6\text{-}C_6Me_6)(bpy)]^+$. Reduction of CO_2 to formate with $[HRu(\eta^6\text{-}C_6Me_6)(bpy)]^+$ is thermodynamically unfavorable by 10 kcal/mol in acetonitrile, but favorable by 2 kcal/mol in water, representing a net change of 12 kcal/mol.[54] The increase in favorability for hydride transfer to CO_2 in water is likely due to hydrogen bonding interactions, which provide greater stabilization for the formate product relative to the metal hydrides. A significant consequence of this trend is that hydrogenation reactions that are thermodynamically unfavorable in acetonitrile may become favorable in water. More importantly, it may lead to the desired hydride transfer reactivity in a more benign solvent for transition metal donors.

CONCLUSION

We have determined the hydricity of a nickel hydride in water, acetonitrile, and DMSO using a thermodynamic cycle benchmarked on the heterolytic bond cleavage energy of H_2. The study represents the first time this value has been determined in three different solvents for the same transition metal hydride donor, and provides a quantitative view of solvation effects. These experimental values are important for benchmarking computational models to more accurately predict solvation effects on heterolytic bond cleavage energies.

When these values are compared to the hydricities of H_2 and HCO_2^- for the three solvents, a significant narrowing of the hydricity range occurs with increasingly polar solvents. However, a nonlinear change in relative hydricities of the metal hydride and HCO_2^- occurs between water and the nonprotic organic solvents, resulting in changes in the thermodynamic favorability (free energy) for hydride transfer.

These hydricity values and their comparisons by solvent are valuable to the design and optimization of catalysts with hydride transfer steps. The results also have broad implications for the general reactivity of transition metal hydrides by revealing how solvent effects can be utilized to promote the desired reactivity.

EXPERIMENTAL SECTION

General Considerations. All manipulations were carried out using standard Schlenk or glovebox techniques under an atmosphere of dinitrogen. Manipulations involving protic solvents were performed in a separate glovebox than those with nonprotic solvents. Solvents were degassed by sparging with argon gas and dried by passage through columns of activated alumina or molecular sieves. Deuterated solvents were purchased from Cambridge Isotopes Laboratories, Inc. and were degassed and stored over activated 3 Å molecular sieves prior to use. Reagents were purchased from commercial vendors and used without further purification unless otherwise noted. $[Ni(NCMe)_{6.5}][BF_4]_2$,[77] $[Ni(PNP)_2][BF_4]_2$,[12] and $[Ni(depp)_2][BF4]_2$,[24] were synthesized according to literature procedures.

Physical Methods. ^1H, ^{13}C, and ^{31}P nuclear magnetic resonance (NMR) spectra were collected at room temperature, unless otherwise noted, on a Bruker AVANCE 600 MHz spectrometer. Chemical shifts reported in δ notation in parts per million (ppm). ^1H and ^{13}C spectra were referenced to TMS at 0 ppm via the residual proteo or natural abundance ^{13}C solvent resonances. ^{31}P spectra were referenced to H_3PO_4 at 0 ppm within Bruker's Topspin 3.2 software, which derives the chemical shifts from the known frequency ratios (Ξ) of the ^{31}P standard to the lock signal of the deuterated solvent.[78] ^{31}P spectra used in determining equilibrium concentration were obtained either with only one pulse or with long delay times (15 s) to ensure quantitative integration. Automatic shimming, Fourier transformation, and automatic spectrum phasing were performed using Bruker's Topspin software. Spectra were worked up and figures were generated using MestReNova 6.0.2 software. Peak integrations were performed either manually or, for determination of equilibrium concentrations, using the peak fitting functionality within MestReNova.

X-ray diffraction studies were carried out at the UCI Department of Chemistry X-ray Crystallography Facility on a Bruker SMART APEX II diffractometer. Data were collected at 100 K using Mo Kα radiation (λ = 0.71073 Å). A full sphere of data was collected for each crystal structure. The APEX2[79] program suite was used to determine unit-cell parameters and to collect data. The raw frame data were processed and absorption corrected using the SAINT[79] and SADABS[80] programs, respectively, to yield the reflection data files. Structures were solved by direct methods using SHELXS and refined against F^2 on all data by full-matrix least-squares with SHELXTL.[81] All non-hydrogen atoms were refined anisotropically. Nonhydroxyl hydrogen atoms were placed at geometrically calculated positions and refined using a riding model, and their isotropic displacement parameters were fixed at 1.2 (1.5 for methyl groups) times the Ueq of the atoms to which they are bonded. Ligand hydroxyl hydrogen atoms were located in the difference map, and their positions and displacement parameters were refined freely.

Cyclic voltammetry was performed on a Pine Wavedriver 10 potentiostat with AfterMath software, using 1 mm diameter glassy carbon disc working electrodes and glassy carbon rod auxiliary electrodes. A pseudoreference electrode with silver wire in 0.2 M

DOI: 10.1021/jacs.5b07777
J. Am. Chem. Soc. 2015, 137, 14114−14121

$[Bu_4N][BF_4]$ separated from the bulk solution by a Vycor tip were used in addition to an internal ferrocene reference. Unless otherwise specified in the text, electrochemistry was performed on 5 mM solutions of analyte with 0.2 M $[Bu_4N][BF_4]$ supporting electrolyte.

Elemental analyses (EA) were performed on a PerkinElmer 2400 Series II CHNS instrument.

Thermodynamic Determinations. *Hydricity (ΔG_{H^-}) in Acetonitrile, DMSO, and Water.* Method 1, via heterolytic cleavage of H_2: Three different amounts of base were added to $[Ni(DHMPE)_2][BF_4]_2$ in the deuterated solvent of interest in a J. Young NMR tube (see SI for reagent concentrations and identity, equivalents, and concentrations of bases used). Method 2, via protonation of the hydride to release H_2 (only for DMSO and water): $Ni(DHMPE)_2$ was dissolved in the deuterated solvent of interest in a J. Young NMR tube. Three different amounts of $[PhNH_3][BF_4]$ (0.1 M in the respective solvent) were added to generate one equivalent of $[HNi(DHMPE)_2][BF_4]$ with various additional equivalents of acid remaining (see SI for equivalents of acid used). For both methods, organic samples were freeze−pump−thawed three times to remove dissolved gases and backfilled with 1 atm H_2, while aqueous samples were vigorously bubbled with water-saturated H_2 for 5 min. The samples were allowed to equilibrate at room temperature for at least 48 h. The relative amounts of $[Ni(DHMPE)_2][BF_4]_2$ to $[HNi(DHMPE)_2][BF_4]$ were monitored by integration of their ^{31}P resonances by NMR spectroscopy until they stabilized. In cases where eventual decomposition was observed, the ratios before significant decomposition were used for hydricity calculations. See Supporting Information for details of hydricity calculations.

pK_a of 3 in DMSO and Water. $Ni(DHMPE)_2$ was dissolved in the deuterated solvent of interest (2 mM for DMSO, 0.02 M for D_2O) and transferred to an NMR tube. In DMSO, 0.5, 1, or 2 equiv of $[HNEt_3][BF_4]$ (0.1 M in DMSO, pK_a = 9.00)) was added via microsyringe and allowed to equilibrate at room temperature for about 5 days. In water, water itself acted as the acid. The relative amounts of $Ni(DHMPE)_2$ and $[HNi(DHMPE)_2][BF_4]$ were then determined by integration of the ^{31}P NMR resonances. See Supporting Information for details of pK_a calculations.

Hydride Transfer in CH_3CN. Equimolar amounts of a hydride of known hydricity and $[Ni(DHMPE)_2][BF_4]_2$ were dissolved in acetonitrile, mixed, and allowed to equilibrate at room temperature for about 18 h. The relative amounts of each species in solution were then determined by integration of their ^{31}P resonances by NMR spectroscopy.

Synthesis. *DHMPE.* Alternative synthetic preparations for this ligand have been reported.[64,65] Under a dinitrogen atmosphere, 1,2-bis(phosphino)ethane (111 mg, 1.21 mmol, 1 equiv) was dissolved in ca. 30 mL methanol in a round-bottom flask. Paraformaldehyde (144 mg, 4.80 mmol, 3.97 equiv) was added as a solid under a flow of nitrogen. The resulting mixture was heated to 80 °C for 48 h with stirring, after which it was cooled to room temperature and the solvents were removed under vacuum. The resulting white residue was triturated and washed with diethyl ether to afford DHMPE as a white solid (164 mg, 64%). ^1H NMR (D_2O, δ): 4.07 (q, J = 13.3 Hz, 8H, PCH_2OH), 1.75 (s, 4H, $R_2PCH_2CH_2PR_2$). Hydroxyl protons not observed in water. $^{31}P\{^1H\}$ NMR (D_2O, δ): −20.8 (s).

*$[Ni(DHMPE)_2][BF4]_2$ (**1**).* Under a dinitrogen atmosphere, $[Ni(NCMe)_{6.5}][BF_4]_2$ (200 mg, 400 μmol, 1 equiv) was dissolved in MeCN and added to a suspension of DHMPE (172 mg, 800 μmol, 2 equiv) in MeCN. The resulting red-orange solution was stirred at room temperature overnight. The reaction was then filtered and volatiles were removed under vacuum from the filtrate, resulting in a red-orange residue. The residue was triturated three times with Et_2O then dried under vacuum to afford $[Ni(DHMPE)_2][BF_4]_2$ as an orange solid (266 mg, 95%).

^1H NMR (CD_3CN, δ): 4.34 (dd, J = 64.4 Hz, J = 13.5 Hz, 16H, PCH_2OH), 3.97 (s, 8H, PCH_2OH), 2.23 (s, 8H, $R_2PCH_2CH_2PR_2$). $^{13}C\{^1H\}$ NMR (CD_3CN, δ): 58.5 (s, PCH_2OH), 20.0 (s, $R_2PCH_2CH_2PR_2$). $^{31}P\{^1H\}$ NMR (CD_3CN, δ): 67.1 (s).

^1H NMR (DMSO-d_6, δ): 5.89 (s, 8H, PCH_2OH), 4.26 (dd, J = 42.0 Hz, J = 13.3 Hz, 16H, PCH_2OH), 2.12 (s, 8H, $R_2PCH_2CH_2PR_2$). $^{13}C\{^1H\}$ NMR (DMSO-d_6, δ): 55.8 (s, PCH_2OH), 17.4 (s, $R_2PCH_2CH_2PR_2$). $^{31}P\{^1H\}$ NMR (DMSO-d_6, δ): 66.8 (s).

^1H NMR (D_2O, δ): 4.51 (dd, J = 38.6 Hz, J = 13.7 Hz, 16H, PCH_2OH), 2.37 (s, 8H, $R_2PCH_2CH_2PR_2$). Hydroxyl resonances not observed in water. $^{13}C\{^1H\}$ NMR (D_2O, δ): 56.7 (s, PCH_2OH), 18.7 (s, $R_2PCH_2CH_2PR_2$). $^{31}P\{^1H\}$ NMR (D_2O, δ): 65.2 (s).

Anal. Calc'd for $C_{12}H_{32}B_2F_8NiO_8P_4$: C, 21.82; H, 4.88. Found: C, 22.20; H, 4.93.

*$Ni(DHMPE)_2$ (**2**).* Method 1: Under a dinitrogen atmosphere, $Ni(PPh_3)_4$ (132 mg, 120 μmol, 1.2 equiv) was dissolved in THF and added to a suspension of DHMPE (43 mg, 200 μmol, 2 equiv) in THF. The resulting suspension was stirred at room temperature overnight, resulting in a gray-purple solid suspended in a yellow solution. The reaction was then filtered and the solid washed with THF then dried under vacuum to afford $Ni(DHMPE)_2$ as a dull purple solid (32 mg, 65%). Method 2: Under a dinitrogen atmosphere, $[Ni(DHMPE)_2][BF_4]_2$ (78 mg, 118 μmol, 1 equiv) was dissolved in MeCN, cooled to −35 °C, then added to a cooled MeCN solution of $CoCp_2$ (49 mg, 259 μmol, 2.2 equiv), resulting in immediate precipitation of a tan solid from the dark brown solution. The suspension was stirred at room temperature for 20 min then filtered, and the solid washed with MeCN and Et_2O then dried under vacuum to afford $Ni(DHMPE)_2$ as a brown solid (42 mg, 74%).

^1H NMR (DMSO-d_6, δ): 4.70 (s, 8H, PCH_2OH), 3.55 (dd, J = 34.1 Hz, J = 10.9 Hz, 16H, PCH_2OH), 1.43 (s, 8H, $R_2PCH_2CH_2PR_2$). $^{13}C\{^1H\}$ NMR (DMSO-d_6, δ): 61.4 (s, PCH_2OH), 21.0 (s, $R_2PCH_2CH_2PR_2$). $^{31}P\{^1H\}$ NMR (DMSO-d_6, δ): 55.8 (s).

^1H NMR (D_2O, δ): 3.89 (br s, 16H, PCH_2OH), 1.71 (br s, 8H, $R_2PCH_2CH_2PR_2$). Hydroxyl resonances not observed in water. $^{13}C\{^1H\}$ NMR (D_2O, δ): 60.8 (s, PCH_2OH), 21.5 (s, $R_2PCH_2CH_2PR_2$). $^{31}P\{^1H\}$ NMR (D_2O, δ): 53.8 (s). Note: The Ni(0) compound **2** is protonated in water to produce the Ni(II) hydride compound **3** (see Results and Supporting Information) over several hours.

Anal. Calc'd for $C_{12}H_{32}NiO_8P_4 + 0.2(CH_3CN)$: C, 30.08; H, 6.64; N, 0.57. Found: C, 30.03; H, 6.28; N, 0.61.

*$[HNi(DHMPE)_2][BF4]$ (**3**).* Method 1: Under a dinitrogen atmosphere, $LiHCO_2{\cdot}H_2O$ (224 μL, 67 mM in DMSO, 15 μmol, 1 equiv) was added to a solution of $[Ni(DHMPE)_2][BF_4]_2$ (10 mg, 15 μmol, 1 equiv) in DMSO to produce an orange-yellow solution of $[HNi(DHMPE)_2][BF_4]$. Method 2: Under a dinitrogen atmosphere, $Ni(DHMPE)_2$ (17 mg, 35 μmol, 1 equiv) was dissolved in ca. 0.5 mL water. To this solution was added a 0.2 M solution of $[PhNH_3][BF_4]$ (157 μL, 31 μmol, 0.9 equiv). The solvent was removed from the resulting yellow-brown solution under vacuum, and the remaining residue was triturated and washed with Et_2O and benzene to afford $[HNi(DHMPE)_2][BF_4]$ as a brown solid (5 mg, 28%).

^1H NMR (CD_3CN, δ): 3.84 (s, 8H, PCH_2OH), 3.97 (m, 16H, PCH_2OH), 1.89 (s, 8H, $R_2PCH_2CH_2PR_2$), −13.47 (pent, $^2J_{P-H}$ = 6 Hz, 1H, HNi). $^{13}C\{^1H\}$ NMR (CD_3CN, δ): 61.0 (s, PCH_2OH), 21.8 (s, $R_2PCH_2CH_2PR_2$). $^{31}P\{^1H\}$ NMR (CD_3CN, δ): 55.6 (s).

^1H NMR (DMSO-d_6, δ): 5.36 (s, 8H, PCH_2OH), 3.86 (m, 16H, PCH_2OH), 1.77 (s, 8H, $R_2PCH_2CH_2PR_2$), −13.43 (pent, $^2J_{P-H}$ = 6 Hz, 1H, HNi). $^{13}C\{^1H\}$ NMR (DMSO-d_6, δ): 58.5 (s, PCH_2OH), 19.2 (s, $R_2PCH_2CH_2PR_2$). $^{31}P\{^1H\}$ NMR (DMSO-d_6, δ): 57.5 (s).

^1H NMR (D_2O, δ): 4.11 (br s, 16H, PCH_2OH), 2.00 (br s, 8H, $R_2PCH_2CH_2PR_2$). Hydroxyl and hydride resonances not observed in water. $^{13}C\{^1H\}$ NMR (D_2O, δ): 59.0 (s, PCH_2OH), 19.9 (s, $R_2PCH_2CH_2PR_2$). $^{31}P\{^1H\}$ NMR (D_2O, δ): 54.7 (s).

■ ASSOCIATED CONTENT

Supporting Information

The Supporting Information is available free of charge on the ACS Publications website at DOI: 10.1021/jacs.5b07777.

DOI: 10.1021/jacs.5b07777
J. Am. Chem. Soc. 2015, 137, 14114−14121

Crystallographic data and tables, NMR spectra, scan rate dependent cyclic voltammetry, and details of thermodynamic calculations (PDF)
cif file (CCDC 1414522) (CIF)

AUTHOR INFORMATION

Corresponding Author

*j.yang@uci.edu

Notes

The authors declare no competing financial interest.

ACKNOWLEDGMENTS

The authors would like to dedicate this publication to the memory of Dr. Carol Creutz, whose research inspired this study. The authors would also like to thank Dr. Aaron Appel for helpful discussions. This material is based on work supported by the U.S. Department of Energy, Office of Science, Office of Basic Energy Sciences under Award Number DE-SC0012150.

REFERENCES

(1) Jacobsen, G. M.; Yang, J. Y.; Twamley, B.; Wilson, A. D.; Bullock, R. M.; Rakowski DuBois, M.; DuBois, D. L. *Energy Environ. Sci.* **2008**, *1*, 167−174.
(2) Capon, J.-F.; Ezzaher, S.; Gloaguen, F.; Pétillon, F. Y.; Schollhammer, P.; Talarmin, J. *Chem. - Eur. J.* **2008**, *14*, 1954−1964.
(3) Bullock, R. M.; Appel, A. M.; Helm, M. L. *Chem. Commun.* **2014**, *50*, 3125−3143.
(4) Sullivan, B. P.; Meyer, T. J. *Organometallics* **1986**, *5*, 1500−1502.
(5) Gibson, D. H.; He, H. *Chem. Commun.* **2001**, 2082−2083.
(6) Bianchini, C.; Ghilardi, C. A.; Meli, A.; Midollini, S.; Orlandini, A. *Inorg. Chem.* **1985**, *24*, 924−931.
(7) DuBois, D. L.; Berning, D. E. *Appl. Organomet. Chem.* **2000**, *14*, 860−862.
(8) Miller, A. J. M.; Labinger, J. A.; Bercaw, J. E. *Organometallics* **2011**, *30*, 4308−4314.
(9) Jeletic, M. S.; Mock, M. T.; Appel, A. M.; Linehan, J. C. *J. Am. Chem. Soc.* **2013**, *135*, 11533−11536.
(10) Creutz, C.; Chou, M. H. *J. Am. Chem. Soc.* **2007**, *129*, 10108−10109.
(11) Appel, A. M.; Bercaw, J. E.; Bocarsly, A. B.; Dobbek, H.; DuBois, D. L.; Dupuis, M.; Ferry, J. G.; Fujita, E.; Hille, R.; Kenis, P. J. A.; Kerfeld, C. A.; Morris, R. H.; Peden, C. H. F.; Portis, A. R.; Ragsdale, S. W.; Rauchfuss, T. B.; Reek, J. N. H.; Seefeldt, L. C.; Thauer, R. K.; Waldrop, G. L. *Chem. Rev.* **2013**, *113*, 6621−6658.
(12) Curtis, C. J.; Miedaner, A.; Ciancanelli, R.; Ellis, W. W.; Noll, B. C.; Rakowski DuBois, M.; DuBois, D. L. *Inorg. Chem.* **2003**, *42*, 216−227.
(13) Henry, R. M.; Shoemaker, R. K.; DuBois, D. L.; DuBois, M. R. *J. Am. Chem. Soc.* **2006**, *128*, 3002−3010.
(14) Wilson, A. D.; Newell, R. H.; McNevin, M. J.; Muckerman, J. T.; Rakowski DuBois, M.; DuBois, D. L. *J. Am. Chem. Soc.* **2006**, *128*, 358−366.
(15) Wilson, A. D.; Shoemaker, R. K.; Miedaner, A.; Muckerman, J. T.; DuBois, D. L.; DuBois, M. R. *Proc. Natl. Acad. Sci. U. S. A.* **2007**, *104*, 6951−6956.
(16) Yang, J. Y.; Smith, S. E.; Liu, T.; Dougherty, W. G.; Hoffert, W. A.; Kassel, W. S.; DuBois, M. R.; DuBois, D. L.; Bullock, R. M. *J. Am. Chem. Soc.* **2013**, *135*, 9700−9712.
(17) Yuki, M.; Sakata, K.; Hirao, Y.; Nonoyama, N.; Nakajima, K.; Nishibayashi, Y. *J. Am. Chem. Soc.* **2015**, *137*, 4173−4182.
(18) Galan, B. R.; Schöffel, J.; Linehan, J. C.; Seu, C.; Appel, A. M.; Roberts, J. A. S.; Helm, M. L.; Kilgore, U. J.; Yang, J. Y.; DuBois, D. L.; Kubiak, C. P. *J. Am. Chem. Soc.* **2011**, *133*, 12767−12779.
(19) Galan, B. R.; Reback, M. L.; Jain, A.; Appel, A. M.; Shaw, W. J. *Eur. J. Inorg. Chem.* **2013**, *2013*, 5366−5371.
(20) Seu, C. S.; Appel, A. M.; Doud, M. D.; DuBois, D. L.; Kubiak, C. P. *Energy Environ. Sci.* **2012**, *5*, 6480−6490.
(21) Teets, T. S.; Nocera, D. G. *J. Am. Chem. Soc.* **2011**, *133*, 17796−17806.
(22) Teets, T. S.; Cook, T. R.; McCarthy, B. D.; Nocera, D. G. *J. Am. Chem. Soc.* **2011**, *133*, 8114−8117.
(23) Darmon, J. M.; Raugei, S.; Liu, T.; Hulley, E. B.; Weiss, C. J.; Bullock, R. M.; Helm, M. L. *ACS Catal.* **2014**, *4*, 1246−1260.
(24) Curtis, C. J.; Miedaner, A.; Ellis, W. W.; DuBois, D. L. *J. Am. Chem. Soc.* **2002**, *124*, 1918−1925.
(25) Galan, B. R.; Wiedner, E. S.; Helm, M. L.; Linehan, J. C.; Appel, A. M. *Organometallics* **2014**, *33*, 2287−2294.
(26) Berning, D. E.; Noll, B. C.; DuBois, D. L. *J. Am. Chem. Soc.* **1999**, *121*, 11432−11447.
(27) Ellis, W. W.; Miedaner, A.; Curtis, C. J.; Gibson, D. H.; DuBois, D. L. *J. Am. Chem. Soc.* **2002**, *124*, 1926−1932.
(28) Ciancanelli, R.; Noll, B. C.; DuBois, D. L.; DuBois, M. R. *J. Am. Chem. Soc.* **2002**, *124*, 2984−2992.
(29) Price, A. J.; Ciancanelli, R.; Noll, B. C.; Curtis, C. J.; DuBois, D. L.; DuBois, M. R. *Organometallics* **2002**, *21*, 4833−4839.
(30) Curtis, C. J.; Miedaner, A.; Raebiger, J. W.; DuBois, D. L. *Organometallics* **2004**, *23*, 511−516.
(31) Ellis, W. W.; Ciancanelli, R.; Miller, S. M.; Raebiger, J. W.; Rakowski DuBois, M.; DuBois, D. L. *J. Am. Chem. Soc.* **2003**, *125*, 12230−12236.
(32) Ellis, W. W.; Raebiger, J. W.; Curtis, C. J.; Bruno, J. W.; DuBois, D. L. *J. Am. Chem. Soc.* **2004**, *126*, 2738−2743.
(33) Raebiger, J. W.; Miedaner, A.; Curtis, C. J.; Miller, S. M.; Anderson, O. P.; DuBois, D. L. *J. Am. Chem. Soc.* **2004**, *126*, 5502−5514.
(34) Miedaner, A.; Raebiger, J. W.; Curtis, C. J.; Miller, S. M.; DuBois, D. L. *Organometallics* **2004**, *23*, 2670−2679.
(35) Raebiger, J. W.; DuBois, D. L. *Organometallics* **2005**, *24*, 110−118.
(36) DuBois, D. L.; Blake, D. M.; Miedaner, A.; Curtis, C. J.; DuBois, M. R.; Franz, J. A.; Linehan, J. C. *Organometallics* **2006**, *25*, 4414−4419.
(37) Fraze, K.; Wilson, A. D.; Appel, A. M.; Rakowski DuBois, M.; DuBois, D. L. *Organometallics* **2007**, *26*, 3918−3924.
(38) Appel, A. M.; Lee, S.-J.; Franz, J. A.; DuBois, D. L.; DuBois, M. R. *J. Am. Chem. Soc.* **2009**, *131*, 5224−5232.
(39) Mock, M. T.; Potter, R. G.; Camaioni, D. M.; Li, J.; Dougherty, W. G.; Kassel, W. S.; Twamley, B.; DuBois, D. L. *J. Am. Chem. Soc.* **2009**, *131*, 14454−14465.
(40) Wilson, A. D.; Miller, A. J. M.; DuBois, D. L.; Labinger, J. A.; Bercaw, J. E. *Inorg. Chem.* **2010**, *49*, 3918−3926.
(41) Roberts, J. A. S.; Appel, A. M.; DuBois, D. L.; Bullock, R. M. *J. Am. Chem. Soc.* **2011**, *133*, 14604−14613.
(42) Estes, D. P.; Vannucci, A. K.; Hall, A. R.; Lichtenberger, D. L.; Norton, J. R. *Organometallics* **2011**, *30*, 3444−3447.
(43) Hu, Y.; Norton, J. R. *J. Am. Chem. Soc.* **2014**, *136*, 5938−5948.
(44) Fong, H.; Peters, J. C. *Inorg. Chem.* **2015**, *54*, 5124−5135.
(45) Kilgore, U. J.; Roberts, J. A. S.; Pool, D. H.; Appel, A. M.; Stewart, M. P.; DuBois, M. R.; Dougherty, W. G.; Kassel, W. S.; Bullock, R. M.; DuBois, D. L. *J. Am. Chem. Soc.* **2011**, *133*, 5861−5872.
(46) Rakowski DuBois, M.; DuBois, D. L. *Chem. Soc. Rev.* **2009**, *38*, 62−72.
(47) Rakowski Dubois, M.; Dubois, D. L. *Acc. Chem. Res.* **2009**, *42*, 1974−1982.
(48) Yang, J. Y.; Bullock, R. M.; Shaw, W. J.; Twamley, B.; Fraze, K.; DuBois, M. R.; DuBois, D. L. *J. Am. Chem. Soc.* **2009**, *131*, 5935−5945.
(49) Das, P.; Ho, M.-H.; O'Hagan, M.; Shaw, W. J.; Morris Bullock, R.; Raugei, S.; Helm, M. L. *Dalton Trans.* **2014**, *43*, 2744−2754.
(50) Moret, S.; Dyson, P. J.; Laurenczy, G. *Nat. Commun.* **2014**, *5*, 4017.
(51) Kang, P.; Cheng, C.; Chen, Z.; Schauer, C. K.; Meyer, T. J.; Brookhart, M. *J. Am. Chem. Soc.* **2012**, *134*, 5500−5503.

DOI: 10.1021/jacs.5b07777
J. Am. Chem. Soc. 2015, 137, 14114−14121

(52) Taheri, A.; Thompson, E. J.; Fettinger, J. C.; Berben, L. A. *ACS Catalysis* **2015**, DOI: 10.1021/acscatal.5b01708.
(53) Taheri, A.; Berben, L. A. Submitted.
(54) Matsubara, Y.; Fujita, E.; Doherty, M. D.; Muckerman, J. T.; Creutz, C. *J. Am. Chem. Soc.* **2012**, *134*, 15743−15757.
(55) Creutz, C.; Chou, M. H. *J. Am. Chem. Soc.* **2009**, *131*, 2794−2795.
(56) Muckerman, J. T.; Achord, P.; Creutz, C.; Polyansky, D. E.; Fujita, E. *Proc. Natl. Acad. Sci. U. S. A.* **2012**, *109*, 15657−15662.
(57) Qi, X.-J.; Fu, Y.; Liu, L.; Guo, Q.-X. *Organometallics* **2007**, *26*, 4197−4203.
(58) Kovács, G.; Pápai, I. *Organometallics* **2006**, *25*, 820−825.
(59) Chen, S.; Rousseau, R.; Raugei, S.; Dupuis, M.; DuBois, D. L.; Bullock, R. M. *Organometallics* **2011**, *30*, 6108−6118.
(60) Raugei, S.; DuBois, D. L.; Rousseau, R.; Chen, S.; Ho, M.-H.; Bullock, R. M.; Dupuis, M. *Acc. Chem. Res.* **2015**, *48*, 248−255.
(61) Kang, S.-B.; Cho, Y.-S.; Hwang, S.-G. *Bull. Korean Chem. Soc.* **2009**, *30*, 2927−2929.
(62) Cho, Y.-S. L.; Lee, J.-B.; Hwang, S.-G. *Bull. Korean Chem. Soc.* **2012**, *33*, 1413−1415.
(63) Nimlos, M. R.; Chang, C. H.; Curtis, C. J.; Miedaner, A.; Pilath, H. M.; DuBois, D. L. *Organometallics* **2008**, *27*, 2715−2722.
(64) Reddy, V. S.; Katti, K. V.; Barnes, C. L. *Inorg. Chim. Acta* **1995**, *240*, 367−370.
(65) Nieckarz, G. F.; Weakley, T. J. R.; Miller, W. K.; Miller, B. E.; Lyon, D. K.; Tyler, D. R. *Inorg. Chem.* **1996**, *35*, 1721−1724.
(66) Addison, A. W.; Rao, T. N.; Reedijk, J.; van Rijn, J.; Verschoor, G. C. *J. Chem. Soc., Dalton Trans.* **1984**, 1349−1356.
(67) Wayner, D. D. M.; Parker, V. D. *Acc. Chem. Res.* **1993**, *26*, 287−294.
(68) Kelly, C. A.; Rosseinsky, D. R. *Phys. Chem. Chem. Phys.* **2001**, *3*, 2086−2090.
(69) Connelly, S. J.; Wiedner, E. S.; Appel, A. M. *Dalton Trans.* **2015**, *44*, 5933−5938.
(70) Nachod, F. C.; Braude, E. A. *Determination of Organic Structures by Physical Methods*; Academic Press: New York, 1955.
(71) Ballinger, P.; Long, F. A. *J. Am. Chem. Soc.* **1960**, *82*, 795−798.
(72) Benoit, R. L.; Mackinnon, M. J.; Bergeron, L. *Can. J. Chem.* **1981**, *59*, 1501−1504.
(73) Asghar, B. H. M.; Crampton, M. R. *Org. Biomol. Chem.* **2005**, *3*, 3971−3978.
(74) Kolthoff, I. M.; Chantooni, M. K.; Bhowmik, S. *J. Am. Chem. Soc.* **1968**, *90*, 23−28.
(75) Crampton, M. R.; Robotham, I. A. *J. Chem. Res., Synop.* **1997**, 22−23.
(76) Kaljurand, I.; Kütt, A.; Sooväli, L.; Rodima, T.; Mäemets, V.; Leito, I.; Koppel, I. A. *J. Org. Chem.* **2005**, *70*, 1019−1028.
(77) Hathaway, B. J.; Holah, D. G.; Underhill, A. E. *J. Chem. Soc.* **1962**, 2444−2448.
(78) Harris, R. K.; Becker, E. D.; Cabral de Menezes, S. M.; Granger, P.; Hoffman, R. E.; Zilm, K. W. *Pure Appl. Chem.* **2008**, *80*, 59−84.
(79) *APEX2*, Version 2014.11; Bruker AXS, Inc.; Madison, WI, 2014.
(80) Sheldrick, G. M. *SADABS*, Version 2014/5; Bruker AXS, Inc.; Madison, WI, 2014.
(81) Sheldrick, G. M. *SHELXTL*; Universität Göttingen: Göttingen, Germany, 2000.

DOI: 10.1021/jacs.5b07777
J. Am. Chem. Soc. 2015, 137, 14114−14121